Journal of Science and Technology – Smart Systems and Devices

Volume 36, Issue 3, Month 2026, ppp–ppp

Development of Electrochemical DNA Biosensors Based Highly Ordered Gold Nanoparticle Arrays

Anh Quang Tran[1,*], Phu Dang Nguyen[1], Duc-Tan Tran[2],

[1]Faculty of Control Engineering, Le Quy Don Technical University, Ha Noi, Vietnam
[2]Faculty of Electrical and Electronic Engineering, Phenikaa University, Ha Noi, Vietnam
[*] Corresponding author email: anhquang.tran@lqdtu.edu.vn

Abstract

The analysis of deoxyribonucleic acid (DNA) plays a crucial role in the diagnosis of genetic and DNA-related diseases such as cancer, anaemia, and cystic fibrosis. Conventional techniques, including polymerase chain reaction (PCR) combined with denaturing gradient gel electrophoresis (DGGE), provide high analytical accuracy but are often time-consuming, labour-intensive, and costly. Therefore, there is a need for simpler and more cost-effective detection strategies. In this study, we present a nanostructured electrochemical platform for DNA detection based on a highly ordered gold nanoparticle (AuNP) array. The sensing mechanism relies on electrochemical impedance spectroscopy (EIS) to monitor DNA structural changes in real time without labelling. Chemically induced denaturation of double-stranded DNA was investigated to evaluate the sensing performance. A significant impedance variation of approximately 20% was observed during the denaturation process, demonstrating the sensitivity of the AuNP-based platform to DNA conformational changes. These results confirm the feasibility of using ordered AuNP arrays combined with EIS as a simple, label-free, and cost-effective approach for monitoring DNA interactions, offering promising potential for biomedical diagnostic applications.

Keywords: Block copolymers, DNA biosensors, EIS biosensors, gold nanoparticles, ordered nanoparticles.

1. Introduction

The identification of specific deoxyribonucleic acid (DNA) sequences plays a crucial role in modern biomedical diagnostics, environmental monitoring, and genetic research. The ability to detect pathogen-specific nucleic acid sequences enables early disease diagnosis and supports the selection of appropriate therapeutic strategies [1]. Moreover, DNA analysis is widely applied in mutation screening, gene expression profiling, and comparative studies between healthy and diseased tissues [2, 3]. It also can be used as a preventive technique by checking water or food supplies for certain pathogens [4]. Besides, the detection of specific DNA sequences is also needed in mutation research [5]. Therefore, rapid and reliable detection of target DNA sequences is therefore essential in both clinical and research settings.

Techniques used for detecting specific DNA sequences are currently time-consuming, multi-step and expensive. Some examples are denaturation gradient gel electrophoresis [6], Southern blotting [7], and micro arrays [8]. However, most optical detection approaches require labeling, staining, or enzymatic amplification, which increases experimental complexity and may affect measurement reliability. These drawbacks have motivated the development of alternative sensing strategies that are faster, simpler, and label-free.

Electrochemical DNA biosensors have emerged as promising platforms due to their high sensitivity, low cost, portability, and compatibility with miniaturized systems [9, 10]. In particular, electrochemical impedance spectroscopy (EIS) enables label-free and real-time monitoring of interfacial changes occurring during DNA hybridization and denaturation [11, 12]. Because impedance measurements are sensitive to variations in surface charge distribution, dielectric properties, and interfacial capacitance, EIS provides an effective approach for probing biomolecular interactions at electrode surfaces.

Nanostructured materials, especially metallic nanoparticles, offer significant advantages in biosensing applications [13, 14]. Gold nanoparticles (AuNPs) are particularly attractive owing to their excellent electrical conductivity, chemical stability, biocompatibility, and strong affinity for thiol-modified biomolecules [15]. When DNA strands are immobilized onto AuNP surfaces, they remain biologically active while inducing pronounced changes in interfacial electrical properties upon hybridization [16]. Compared with bulk materials, nanoparticle-based platforms amplify surface-related

p-ISSN 3093-3285
e-ISSN 3093-3315
https://doi.org/10.51316/jst.192.ssad.2026.36.x.x
Received: Feb 28, 2026; Revised: Mar 23, 2026;
Accepted: May 15, 2026; Online: June 8, 2026

effects, thereby enhancing sensor sensitivity [17]. Various fabrication methods have been developed to produce metal nanoparticles, including wet-chemical synthesis [18] and cluster-beam deposition [19]. However, these approaches often encounter challenges such as particle aggregation and limited control over spatial ordering. Block copolymer micellar nanolithography provides a powerful alternative for fabricating highly ordered nanoparticle arrays with tunable size and interparticle spacing [20, 21]. This method enables precise control of nanoparticle density, which directly influences the amount and orientation of immobilized DNA strands and thus the sensing performance. The controlled spacing between nanoparticles can also reduce aggregation effects and ensures that probe DNA molecules are distributed more homogeneously across the sensing surface.

Therefore, in this work, we develop a label-free electrochemical DNA biosensor based on a highly ordered AuNP array fabricated on silicon substrates using a micellar approach combined with dip-coating. Thiol-modified probe DNA strands are immobilized onto the AuNP surface without the need for additional linker molecules. The hybridization with complementary DNA (cDNA) and subsequent chemically induced denaturation are monitored in real time using electrochemical impedance spectroscopy. The impedance variation associated with DNA duplex formation and denaturation is used to evaluate the sensing capability of the nanostructured platform.

2. Materials and Methods

2.1. Materials and Instrumentation

In this research, the silicon wafers used as substrates were purchased from WaferNet Inc. (San Jose, California, USA). These wafers were n-type doped Si with a thickness of 525 ± 15 µm and a (111) crystal orientation. Their bulk resistivity ranged from 0.009 to 0.0111 Ω·cm, while the surface roughness was extremely low (RMS ≈ 0.147 nm). The diblock copolymers *PS(32500)-b-P2VP(7800)* were obtained from Polymer Source (Dorval, Canada). The gold precursor salt, $HAuCl_4$, was supplied by Sigma-Aldrich. Thiol-modified probe DNA (5'-HS-CGCATTCAGGATCGC-3') and complementary DNA (5'-GCGATCCTGAATGCG-3') were purchased from Thermo Fisher Scientific (Germany). PCR buffer containing 0.05 M KCl and 0.01 M Tris-HCl (pH 8.3 at room temperature) and sodium dodecyl sulfate (SDS) were obtained from Roche (Belgium) and VWR International (Belgium), respectively. Acetone and isopropanol used for substrate cleaning were purchased from VWR International (Belgium). A 0.01 M MES buffer solution was prepared in the laboratory.

For instrumentation: Electrochemical impedance measurements were carried out using an IviumStat instrument (Ivium Technologies, Eindhoven, The Netherlands). AFM images were obtained with a Nanoscope IIIa system (Germany). Custom-built EIS setups were used for dip-coating, impedance analysis, and characterizations (Vietnam).

2.2 Biosensing Platform Preparation and Characterizations

The biosensing platform was fabricated by forming highly ordered gold nanoparticle (AuNP) arrays on silicon substrates using the block copolymer micellar nanolithography approach. In this method, diblock copolymer micelles act as nanoreactors that confine metal precursors and define the spatial arrangement of nanoparticles.

First, a micellar solution was prepared by dissolving the diblock copolymer *PS(32500)-b-P2VP(7800)* in toluene under continuous stirring. Due to the amphiphilic nature of the copolymer, spherical micelles were formed in the solvent, consisting of a hydrophobic PS corona and a P2VP core. Subsequently, an appropriate amount of gold precursor ($HAuCl_4$) was introduced into the micellar solution. The gold ions selectively coordinated with the P2VP blocks inside the micelle cores, resulting in Au-salt-loaded micelles. The solution was stirred for approximately three days to ensure uniform loading of the precursor within the micelles. Afterward, the solution was filtered to remove possible contaminants and large aggregates.

A monolayer of micelles containing the gold precursor was then transferred onto the cleaned Si substrates using the dip-coating technique. During the withdrawal process, a quasi-hexagonally ordered monolayer of micelles was formed on the surface due to self-assembly and capillary forces. The polymer matrix was subsequently removed by oxygen plasma etching, leaving behind metallic gold nanoparticles anchored on the substrate surface. As a result, a highly ordered array of AuNPs with controlled particle size and interparticle spacing was obtained.

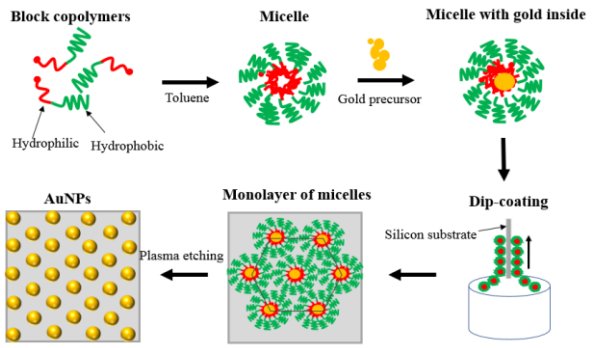

Fig. 1. The schematic of the gold nanoparticle synthesis by the block copolymer nanolithography

The overall fabrication process of the AuNP arrays using block copolymer nanolithography is illustrated in Fig. 1. The quality of the micellar solutions was first checked by AFM imaging before etching the polymer

with the oxygen plasma. Fig. 2 shows the AFM image of micelles and their respective AuNPs produced using the *PS(32500)-b-P2VP(7800)* polymer. Important parameters such as particle sizes, the inter-particle distance, and the distribution of the particles can be determined using the Gwyddion software. The size of AuNPs and their interparticle distance are estimated at 3 nm and 40 nm, respectively. The Fig. 2 illustrates the highly ordered distribution of dip-coated micellular particles (left) and its AuNPs after etching (right). The size of the AuNPs and the interparticle distance are important parameters that will affect the sensitivity of the biosensor. When the size of the AuNPs and the interparticle distance decrease, the number of particles on the same surface area will increase. As a result, the sensitivity of the sensor increases due to the enlargement of the coverage of the AuNPs area.

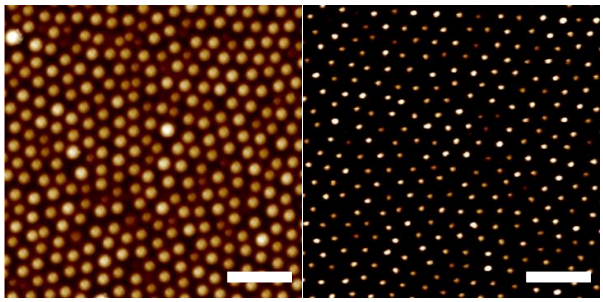

Fig. 2. AFM image of micelles after dip-coating (left) and gold nanoparticles after etching (right) on the same Si substrate from the solution. The scale bar is 100 nm

After depositing the gold nanoparticles on a substrate, DNA will be attached to them. Thiolated (SH)-DNA was used because Thiol has a high affinity for gold. The chemisorption allows binding of SH-terminated DNA to gold without extra preparation of the surface or additional linker molecules to attach DNA, which had been reported in many research groups [22, 23] and our previous study as well [16]. Then, it is necessary to study the target hybridization. Currently, detection techniques that rely on an optical change during hybridization are often used. The optical change induced by the hybridization with fluorescent, chemiluminescent, colorimetric, and other types of labelled probes. The optical signal can also be created indirectly by the use of enzymes. These enzymes then need to generate the appropriate signals [24]. In this study, electrochemical impedance spectroscopy (EIS) was used to measure the electrical resistance (impedance) change at alternating current. This promising technique was used because it is label-free, fast, and real-time measurements. The EIS signals figure out both the attachment of probe DNA and the hybridization, the denaturation of the DNA strands with complementary DNA.

Fig. 3 illustrates the sample preparation processes for studying the chemically induced DNA denaturation. The AuNPs on the substrate was first covered with probe DNAs via thiol groups associated with the probe DNA. The complementary DNA (cDNA) were then hybridized with the probe DNA to from double stranded DNAs (dsDNA). For the small AuNPs of 3 nm and the inter-particle distance of 40 nm, the number of AuNPs is about 490 particles μm^2. If each DNA strand has cross section area of about 2 nm, it is supposed that there will be nearly 500 probe DNA/ μm^2.

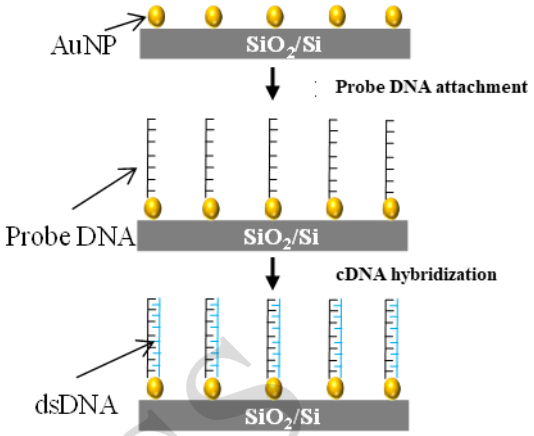

Fig. 3. The illustration of gold nanoparticle-based platform with physisorbed probe DNA before and after hybridization with complementary DNA (cDNA) to form double stranded DNA (dsDNA)

2.3 Electrochemical impedance spectroscopy (EIS) analyzer

Electrical resistance is the ability of a circuit element to resist the flow of electrical current. A known definition of electrical resistance is defined by Ohm's law [25]. However, that law has limited with only ideal resistors. An ideal resistor follows Ohm's law at any current and voltage levels; the resistance level is independent of frequency and AC current and voltage signals are in phase with each other. Many circuit elements have more complex behavior. For these elements, impedance spectroscopy can be used. Impedance is also a measurement of the ability of a circuit element to resist the flow of electrical current.

Impedance can be measured by applying an AC current to a cell and measuring the resulting AC potential. In a pseudo-linear system, created by using a small excitation signal, the response to a sinusoidal current will be a sinusoidal potential at the same frequency but shifted in phase. This phase shift makes impedance a complex quantity (Equation 1). At certain frequencies, the phase shift will be more pronounced [26, 27].

$$Z = Z' + iZ'' \quad (1)$$

Impedance measurements are often analyzed by fitting the data to an equivalent electrical circuit model which contain different connection of resistors, capacitors, and inductors. While the impedance of a capacitor depends on frequency, the impedance of an ideal resistor does not. In this work, the Nyquist spectra

will be interpreted using a modified Randles-type equivalent circuit consisting of the solution resistance (Rs) in series with a parallel combination of the interfacial charge-transfer/polarization resistance (Rct) and a constant phase element (CPE). The use of a CPE instead of an ideal capacitor accounts for the non-ideal capacitive behavior caused by surface heterogeneity, roughness, and distributed time constants on the DNA modified-AuNP array [28]. The impedance measured data will be presented with a Nyquist plot and the impedance values overtime at a certain frequency [26, 27].

The EIS is useful to study with liquid electrolytes, ionically conducting glasses and polymers, fuel cells, corrosion, etcetera. The presence of mobile charges may influence the measurements in several ways, for instance, bulk resistive-capacitive effects, bulk generation-recombination effects, adsorption at electrodes, electrode reactions and diffusion [26, 27]. In this work, the EIS was conducted with the ionic conduction predomination.

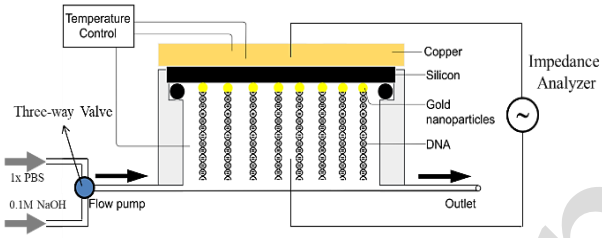

Fig. 4. The schematic model of the homemade impedance spectroscopy device with temperature control and a pumping system used in this research for studying chemically induced DNA denaturation

Fig. 4 illustrates a schematic overview of the EIS using in the experiments. Different fluids are able to pump into the cell using a pumping system and a three-way valve. In this study, phosphate-buffered saline (1x PBS) and 0.1 M NaOH are used, but the solvents can be changed depending on the measurements. The backside of the sample is attached to the copper lid while the front side is exposed to the liquid in the measurement chamber. The working electrode is formed by the dsDNA on nanoparticles dip-coated on highly-doped silicon and the counter electrode is a platinum wire. The two electrodes are connected to an impedance analyzer that allows measuring the impedance change. The temperature inside the fluid and a copper can be monitored and controlled with a thermocouple. The temperature of the liquid inside the chamber is remained constant at 37 ºC during the EIS measurements as shown in Fig. 5. In the experiment, the 0.1M NaOH solution is first pumped into the chamber to induce the chemical DNA denaturation at the speed of 0.1mL/min. After waiting for stability, the 1xPBS buffer is pumped to rinse the denatured ssDNA out of the chamber. Finally, the 0.1M NaOH is pumped again to the chamber for studying the impedance properties of the sensor platform.

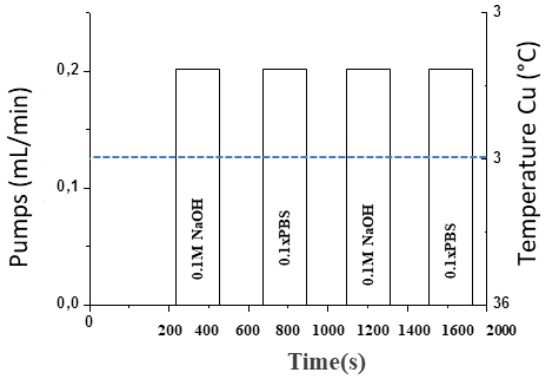

Fig. 5. Graphical representation of the pumping cycle used at an EIS measurement for a sample at different states. The pumping speed is set at 0.125 ml/min for both PBS and NaOH solutions

3. Results and discussions

To understand the impedance properties of the samples and their influence on the EIS measurements, Nyquist plots were carried out by the Iviumstat impedance/gain-phase analyzer. The Nyquist plot is drawn after each EIS measurement for a sample with probe DNA and cDNA. Fig. 6 shows the Nyquist plots with different states of the biosensor platform. It can be seen that there is almost no difference between the bare and AuNP samples. However, when the sample is functionalized with probe DNA and attached, it shows different impedance properties as shown in the Nyquist plots. This result indicates that the introduction of the DNA layer on AuNPs significantly modifies the interfacial electrical properties of the sensing platform, most likely through changes in surface charge distribution, interfacial capacitance, and local ionic transport near the electrode surface. After hybridization with cDNA, the impedance response changes further, suggesting the formation of a double-stranded DNA layer with interfacial characteristics different from those of probe DNA alone.

In addition, a slight difference in impedance is also observed for the same sample before and after the EIS measurement. This effect may be attributed to partial rearrangement of the surface-bound DNA layer during the measurement, minor changes in the interfacial hydration/ion distribution, or small variations in experimental conditions such as solvent exchange and temperature stability inside the measuring chamber. In particular, the use of NaOH and PBS pumping cycles, together with the reported temperature fluctuation at the electrode during the measurement, may contribute to a modest shift in the measured impedance. Therefore, this small before/after difference may not be considered as contradictory to the sensing mechanism, but rather as an indication that the DNA-modified interface remains dynamically responsive to the measurement environment.

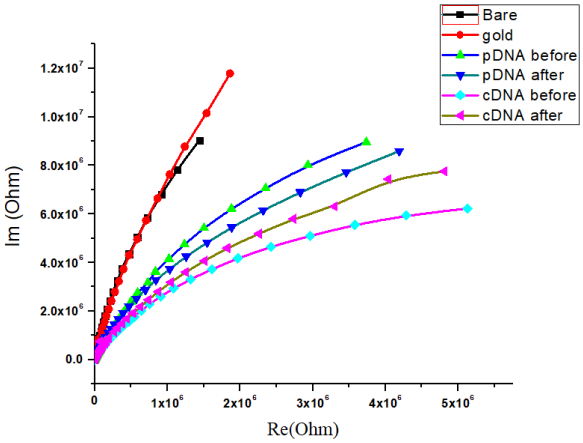

Fig. 6. Nyquist plots are measured for a sample at different steps, made out of data from the Iviumstat impedance/gain-phase analyser device

The EIS measurements were performed for a sample with different preparation steps. First, the bare Silicon sample was measured before it is used for fabricating the AuNPs array. Then, the sample with AuNPs was measured for studying the impedance properties of the sensing platform's surface. In the probe DNA functionalizing step, the AuNPs on the sample was immobilized with probe DNA (ssDNA) and measured with the EIS before being attached with the cDNA at the final step. During the impedance measurements, three different setups were used. The first setup had two chambers. Inside the first chamber, the fluids were pre-heated and inside the second chamber, two samples were measured. The second setup pre-heated the fluids inside a small plastic tube. With this setup a single sample could be measured at one time. The last setup did not provide the pre-heating of incoming fluids. With this setup, it was possible to connect measuring chambers in which one, two or four samples could be measured at a given time.

The pumps of the impedance spectrometer were programmed the same for all measurements at different stages: before, during, and after the denaturation of the DNA (see again in Fig. 5). Each EIS measurement was first performed for the sample inside the chamber with a 0.1x PBS environment for 40 min (step 1). After that 0.1 M NaOH (12 min, 0.25 ml/min) was pumped into the measuring cell (step 2). The NaOH resided for an extra 32 min inside the measuring cell (to ensure complete denaturation of the dsDNAs) (step 3). The cell was then rinsed with 0.1x PBS for 12 min (0.25 ml/min), this washed the denatured DNA off (step 4). The measurement was performed for 32 min with a stable PBS environment (step 5). As a second 0.1 M NaOH was pumped inside the measuring cell (step 6). The second NaOH step is kept stable for measurement to discern between the impedance change caused by the different solvents and that caused by the denaturation of dsDNAs (step 7). Finally, the NaOH was replaced with PBS pumping as step 4 (step 8) and remained 32 min for EIS measurement (step 9). The temperature was kept constant at 37 °C during the entire measurement. During the EIS measurement, the temperature of the Cu-electrode was changed. This temperature change also influences the temperature inside the measuring cell.

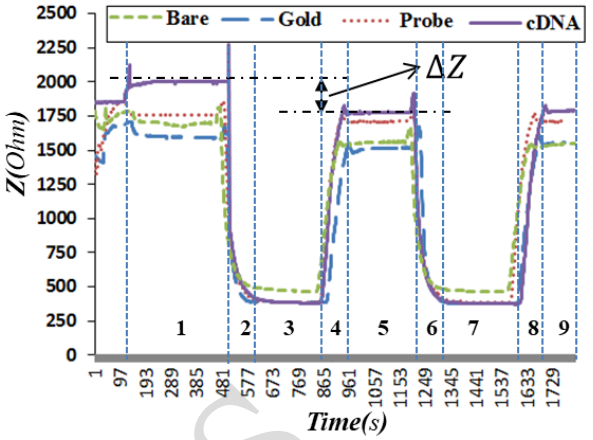

Fig. 7. EIS measurements for a sample at different sample preparation states (bare, gold, probe DNA, cDNA sample). The measurements were performed for different steps of PBS and NaOH pumping (step 1 – step 9). *ΔZ* is the change of impedance

Fig. 7 shows the displacement of the EIS measurements. It can be seen that the impedance reduces significantly and remained stable when the NaOH is pumped and kept in the chamber (steps 2 and 3). After replacing NaOH by pumping the PBS buffer (step 4), the impedance almost increases back to the initial state for bare, AuNP, and probe DNA samples (step 5). The repeating steps of pumping NaOH and PBS did not cause any change in impedance for these samples (step 9). Differently, the sample with cDNA shows a different behaviour with a noticeable decrease in the impedance at step 5. This means the denaturation of dsDNAs on the sample had influenced the impedance properties of the sample, which was not seen on the other samples. The difference impedance, *ΔZ* is approximately 20% lower than the sample with the cDNA before denaturation. After the second NaOH and PBS cycles, the impedance did not change between steps 5 and 9 as seen before. This suggests the occurrence of DNA denaturation, which is consistent with the experimental conditions and the expected dielectric properties of dsDNA and ssDNA. Although a deeper understanding of what causes the change of the impedance is still needed more investigation, it can be explained that the dsDNA on the sensing platform make higher impedance due to their higher dielectric value [29]. After the DNA denaturation process, only the ssDNA (probe DNA) left on the platform has lower dielectric value that leads to reduce the impedance, specifically the capacity between two measuring electrodes.

To further evaluate the reliability and reproducibility of the proposed sensing platform, electrochemical

impedance spectroscopy (EIS) measurements were conducted on two independently prepared samples under identical experimental conditions (Fig. 9). Both samples were functionalized with probe DNA and hybridized with complementary DNA (cDNA) following the same fabrication and measurement protocol.

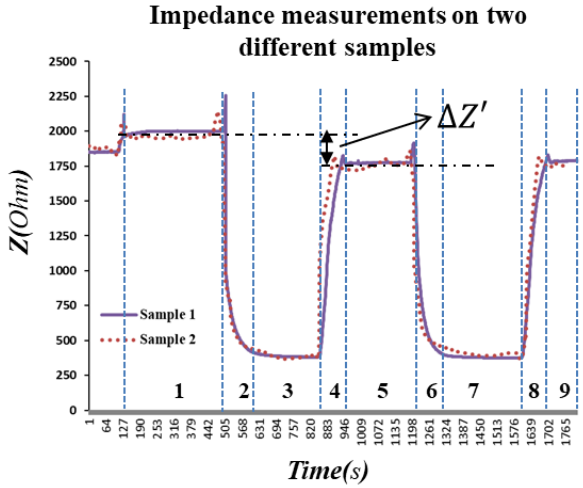

Fig. 8. EIS measurements for 2 different samples prepared by the same method and condition for cDNA (sample 1 and sample 2). The measurements were performed the same as aforementioned procedure with different steps of PBS and NaOH pumping (step 1 – step 9). *ΔZ'* is the change of impedance of sample 2

As observed in Fig. 8, the impedance responses of sample 1 and sample 2 exhibit very similar trends throughout the entire measurement cycle (steps 1–9). In both cases, a high and stable impedance value is initially recorded in the PBS environment (step 1). Upon introduction of NaOH (steps 2–3), a sharp decrease in impedance is observed, corresponding to the chemically induced denaturation of double-stranded DNA (dsDNA). This decrease is followed by a partial recovery when the system is rinsed with PBS (step 4), after which the impedance stabilizes at a lower level compared to the initial state (step 5). This behavior is consistent with the removal of denatured strands and the presence of remaining single-stranded probe DNA on the AuNP surface as seen in the cDNA sample graph (sample 1) shown in the Fig. 7. Importantly, both samples show similar impedance changes (*ΔZ* and *ΔZ'* of about 20%), indicating a high degree of reproducibility in the sensing response. The magnitude of impedance variation during the denaturation process is consistent between the two samples, confirming that the observed signal is not due to random fluctuations or measurement artifacts, but rather originates from the intrinsic physicochemical changes occurring at the DNA-modified electrode interface.

Minor differences between the two sample measurements can be attributed to slight variations in nanoparticle distribution or sample preparation steps, DNA surface coverage, or local experimental conditions, which are inevitable in nanoscale fabrication processes. However, these variations do not significantly affect the overall sensing performance or the qualitative behavior of the system. From these observations, it can be confirmed that the strong agreement between the impedance responses of the two independently prepared samples demonstrates the repeatability and reliability of the proposed AuNP-based electrochemical DNA biosensor. This reproducibility is essential for practical applications, particularly in biomedical diagnostics, where consistent and reliable detection is required.

This research develops a new DNA detection method based on block copolymer nanofabrication and a label-free and real-time EIS measurement with a simple data read-out. Here, gold nanoparticles (AuNPs) with the size of 3 nm were produced in a well-ordered array on Si using the micellar approach and the dip-coating technique as described in our previous study [16]. Then strong chemisorption via Au–S bonds was used to immobilize probe DNA modified with alkyl thiol groups based on their strong and specific affinity. Finally, the hybridization of cDNA with the probe DNA on sensing platform was performed to study the impedance properties of the double stranded DNA (dsDNA) by using chemically induced denaturation. The change in the impedance property on the surface of nanostructure-based sensing platform due to the chemically induced DNA denaturation was used to estimate the sensitivity of the biosensors.

An important aspect of this work is the use of highly ordered gold nanoparticle (AuNP) arrays fabricated by block-copolymer micellar nanolithography, which distinguishes this sensing platform from many previously reported nanoparticle-based biosensors. In conventional nanoparticle deposition methods, nanoparticles are often randomly distributed on the substrate surface, resulting in significant variations in particle density, interparticle distance, and surface coverage. Such structural inhomogeneity can lead to variability in DNA immobilization and reduced reproducibility of the electrochemical response. Nevertheless, our proposed method used in this study enables the formation of hexagonally ordered AuNP arrays with well-controlled nanoparticle size and interparticle spacing. This structural regularity provides a more uniform nanoscale interface for DNA immobilization This highly ordered arrangement of AuNPs is particularly beneficial for impedance-based biosensing as electrochemical impedance spectroscopy is highly sensitive to interfacial properties, a uniform nanoparticle distribution helps produce more stable and reproducible electrical signals. Furthermore, the high density of small 3nm AuNPs increases the effective surface area available for probe DNA attachment, which can enhance the interaction between the sensing interface and target DNA molecules. As a result, this

proposed sensing platform can improve signal consistency and sensitivity in detecting DNA structural changes.

6. Conclusion

In this study, a label-free DNA biosensor based on a highly ordered AuNP array was successfully developed and evaluated by EIS. The ordered nanostructure provided a uniform interface for probe DNA immobilization and enabled clear detection of DNA hybridization and denaturation. The cDNA-hybridized sample showed a characteristic impedance decrease of about 20% after denaturation, while control samples did not exhibit the same behavior. Similar responses obtained from independently prepared samples demonstrated good repeatability of the sensing platform. For the first time, in this study, the use of a highly ordered AuNP array as a reproducible sensing interface for label-free EIS-based DNA detection is developed and evaluated. This platform shows promise for simple and cost-effective biosensing methods, offering promising potential for future electrochemical biosensing applications.

Acknowledgments

This research is supported by the Le Quy Don Technical University in the research projects under Grant No. 4187/QĐ-HV.

References

[1] Huang, T., R. Zhang, and J. Li, CRISPR-Cas-based techniques for pathogen detection: Retrospect, recent advances, and future perspectives. Journal of Advanced Research, vol. 50: pp. 69-82, Aug. 2023. https://doi.org/10.1016/j.jare.2022.10.011

[2] S. Nomura, Single-cell genomics to understand disease pathogenesis. Journal of Human Genetics, vol. 66, iss 1, pp. 75-84, 2021. https://doi.org/10.1038/s10038-020-00844-3

[3] Hekselman, I. and E. Yeger-Lotem, Mechanisms of tissue and cell-type specificity in heritable traits and diseases. Nature Reviews Genetics, vol. 21, iss. 3, pp. 137-150, Mar. 2020. https://doi.org/10.1038/s41576-019-0200-9

[4] Vidic, J., P. Vizzini, M. Manzano, D. Kavanaugh, N. Ramarao, M. Zivkovic, V. Radonic, N. Knezevic, I. Giouroudi, and I. Gadjanski, Point-of-Need DNA Testing for Detection of Foodborne Pathogenic Bacteria. Sensors (Basel, Switzerland), vol. 19, iss. 5, p. 1100, 2019.

[5] Mahdieh, N. and B. Rabbani, An overview of mutation detection methods in genetic disorders. Iranian journal of pediatrics, vol. 23, iss. 4, pp. 375-388, 2023.

[6] J. Vidic, P. Vizzini, M. Manzano, D. Kavanaugh, N. Ramarao, M. Zivkovic, V. Radonic, N. Knezevic, I. Giouroudi, and I. Gadjanski, Agarose gel electrophoresis for the separation of DNA fragments. Journal of visualized experiments : JoVE, vol. 62, p. 3923, Apr. 2020.

[7] E. M. Southern, Detection of specific sequences among DNA fragments separated by gel electrophoresis. Journal of Molecular Biology, vol. 98, iss. 3, pp. 503-517, Nov. 1975. https://doi.org/10.1016/S0022-2836(75)80083-0

[8] Schena, M., D. Shalon, R.W. Davis, and P.O. Brown, Quantitative Monitoring of Gene Expression Patterns with a Complementary DNA Microarray. Science, vol. 70, no. 5235, pp. 467-470, 1995. https://doi.org/10.1126/science.270.5235.467

[9] Bhuiyan, M.S.A., G. Ringgit, S. Sarker, A.M.S. Abu Bakar, S. Saallah, Z. Amin, S.M. Shaarani, and S. Siddiquee, Electrochemical DNA Biosensor for the Detection of Infectious Bronchitis Virus Using a Multi-Walled Carbon Nanotube-Modified Gold Electrode. Poultry, vol. 4, iss 1, p. 12, 2025.

[10] Williamson, P., P. Piskunen, H. Ijäs, A. Butterworth, V. Linko, and D.K. Corrigan, Signal Amplification in Electrochemical DNA Biosensors Using Target-Capturing DNA Origami Tiles. ACS Sensors, vol. 8, iss. 4, pp. 1471-1480, 2023.

[11] Yang, Y., et al., Electrochemical DNA Biosensors with Dual-Signal Amplification Strategy for Highly Sensitive HPV 16 Detection. Sensors, vol. 23, iss. 17, p. 7380, 2023.

[12] Bagherzadeh-Nobari, S. and R. Kalantarinejad, Real-time label-free detection of DNA hybridization using a functionalized graphene field effect transistor: a theoretical study. J Nanopart Res, vol. 23, iss. 8, p. 185, 2021.

[13] Huang, R., N. He, and Z. Li, Recent progresses in DNA nanostructure-based biosensors for detection of tumor markers. Biosensors and Bioelectronics, vol. 109, p. 27-34, 2018.

[14] Roy, S. and Z. Gao, Nanostructure-based electrical biosensors. Nano Today, vol. 4, pp. 318-334, 2009.

[15] C. Miller, K. K. Hussain, O. Keattch, and B. A. Patel, Deposition of gold nanoparticles is varied by different scales of various surface patterns on 3D printed electrodes. Electrochimica Acta, vol. 529, 2025, Art. no. 146401.

[16] A. Q. Tran, The study of thermal stability of dna duplex on nanoparticle-based platforms: a method for biosensing applications. Journal of Science and Technique, vol. 14, iss. 5, 2021.

[17] Liu, B. and J. Liu, Interface-Driven Hybrid Materials Based on DNA-Functionalized Gold Nanoparticles. Matter, vol. 1, iss. 4, pp. 825-847, 2019.

[18] Tatar, D.K. and J.M. Jha, Wet chemical synthesis and characterization of CuO nanoparticles and their application in pool boiling heat transfer. Journal of Crystal Growth, vol. 617, 2023, Art. no. 127305.

[19] Palmer, R.E., R. Cai, and J. Vernieres, Synthesis without Solvents: The Cluster (Nanoparticle) Beam Route to Catalysts and Sensors. Accounts of Chemical Research, vol. 51, iss. 9, pp. 2296-2304, 2018.

[20] J. P. Spartz, S. Mössmer, C. Hartmann, M. Möller, T. Herzog, M. Krieger, H.-G. Boyen, P. Ziemann, and B. Kabius, Ordered deposition of inorganic clusters from

micellar block copolymer films. Langmuir, vol. 16, iss 2, pp. 407-415, 2000.

[21] Bansmann, J., S. Kielbassa, H. Hoster, F. Weigl, H.G. Boyen, U. Wiedwald, P. Ziemann, and R.J. Behm, Controlling the interparticle spacing of Au-salt loaded micelles and Au nanoparticles on flat surfaces. Langmuir, vol. 23, iss. 20, pp. 10150-10155, 2007.

[22] Ma, X., X. Li, G. Luo, and J. Jiao, DNA-functionalized gold nanoparticles: Modification, characterization, and biomedical applications. Front Chem,. vol. 10, pp. 1095488, 2022.

[23] Ghotra, G., B.K. Nguyen, and J.I.L. Chen, DNA-Functionalized Gold Nanoparticles with Toehold-Mediated Strand Displacement for Nucleic Acid Sensors. ACS Applied Nano Materials, vol. 3, iss. 10, pp. 10123-10132, 2020.

[24] Storhoff, J.J., R. Elghanian, R.C. Mucic, C.A. Mirkin, and R.L. Letsinger, One-Pot Colorimetric Differentiation of Polynucleotides with Single Base Imperfections Using Gold Nanoparticle Probes. Journal of the American Chemical Society, vol. 120, iss. 9, pp. 1959-1964, 1998.

[25] Kuphaldt, T.R., Lessons In Electric Circuits. 2006.

[26] Macdonald, J.R., Impedance Spectroscopy. Annals of Biomedical Engineering, vol. 20, pp. 289-305, 1992.

[27] Katz, E. and I. Willner, Probing Biomolecular Interactions at Conductive and Semiconductive Surfaces by Impedance Spectroscopy: Routes to Impedimetric Immunosensors, DNA-Sensors, and Enzyme Biosensors. Electroanalysis, vol 15, iss. 11, pp. 913-947, 2023.

[28] Córdoba-Torres, P., T. Mesquita, and R. Nogueira, Relationship between the Origin of Constant-Phase Element Behavior in Electrochemical Impedance Spectroscopy and Electrode Surface Structure. The Journal of Physical Chemistry C, vol. 119, iss. 8, 2015.

[29] Gruner, G., Conductivity and dielectric constant of the DNA double helix. AIP Conference Proceedings, vol. 544, iss. 1, pp. 462-467, 2000.